Polyhedron 64 (2013) 304–307

Contents lists available at SciVerse ScienceDirect

Polyhedron

journal homepage: www.elsevier.com/locate/poly

# Structural insights into $[Co_4O_4(C_5H_5N)_4(CH_3CO_2)_4]^+$, a rare Co(IV)-containing cuboidal complex

Troy A. Stich [a], J. Krzystek [b], Brandon Q. Mercado [a], J. Gregory McAlpin [a], C. André Ohlin [c], Marilyn M. Olmstead [a], William H. Casey [a,d], R. David Britt [a,*]

[a] Department of Chemistry, University of California, One Shields Avenue, Davis, CA 95616, United States
[b] National High Magnetic Field Laboratory, Florida State University, Tallahassee, FL 32310, United States
[c] School of Chemistry, Monash University, Vic 3800, Australia
[d] Department of Geology, University of California, One Shields Avenue, Davis, CA 95616, United States

ARTICLE INFO

*Article history:*
Received 5 April 2013
Accepted 21 May 2013
Available online 7 June 2013

*Keywords:*
Cobalt
EPR
Water-oxidation

ABSTRACT

We report high-frequency (up to 219 GHz) and correspondingly high-field electron paramagnetic resonance spectra and X-ray crystal structure of $[Co_4O_4(pyridine)_4(acetate)_4]^+$ ($[Co_4O_4(py)_4(OAc)_4]^+$) that serves as a structural and spectroscopic model of cobalt-oxide films that are capable of oxidizing water. These results are, in large part, consistent with those from our earlier, lower-frequency study and serve to benchmark future high-field studies on paramagnetic states of the catalyst film.



## 1. Introduction

Cobalt-oxide films formed on the surface of an electrode have been shown to be potent water oxidation catalysts, splitting water into protons, electrons, and oxygen gas with only a modest overpotential [1]. During catalysis, these films access high oxidation states of the constituent cobalt ions up to $Co^{IV}$ [2]. The proposed structure of the active catalyst likely has incomplete cuboidal $[Co_3O_4]$ motifs (perhaps missing one of the vertex cobalt ions) [3,4]. Thus we have explored the electronic structure of a cuboidal cobalt-oxido species [5] that itself purportedly has water-splitting activity [6–8]. In this report we extend these previous continuous-wave electron paramagnetic resonance (CW EPR) spectroscopic studies to the much higher excitation frequencies and fields available at the National High Magnetic Field Lab in Tallahassee, FL. In addition, we have determined the crystal structure of $[Co_4O_4(py)_4(OAc)_4]^+$ and compare these geometric results to those obtained previously for the reduced form.

## 2. Methods

### 2.1. Synthesis

$[Co_4O_4(py)_4(OAc)_4]$ was synthesized following the literature procedure [5,9]. Electrochemical oxidation of $[Co_4O_4(py)_4(OAc)_4]$ to $[Co_4O_4(py)_4(OAc)_4]^+$ was performed with a Princeton Applied Research Model 263A potentiostat and POWERSTEP software package using the previously published procedures [2]. A potential of up to 1.1 V relative to a $Ag^0$ pseudo-reference electrode was applied to a 5 mM solution of $[Co_4O_4(py)_4(OAc)_4]$ in $CH_3CN$ in the presence of 0.4 M $LiClO_4$. The potential was applied until the current density reached a steady state. The total number of liberated electrons measured was less than one equivalent of the amount of $[Co_4O_4(py)_4(OAc)_4]$ present in solution (≈0.5 charge equivalents), suggesting that each molecule was oxidized by, at most, one electron. The solution was reduced to approximately one-fifth the original volume, titurated with water (20 mL), and refrigerated overnight to facilitate crystal growth.

### 2.2. Crystal structure determination

A green black crystal of dimensions 0.07 × 0.12 × 0.12 mm was mounted in the 90(±2) K nitrogen cold stream provided by a CRYO Industries low temperature apparatus on the goniometer head of a Bruker DUO diffractometer equipped with an ApexII CCD detector. In the structure solution, extensive tests were made to check for alternative space groups, but only $Pmn2_1$ gave a successful refinement. The structure could not be refined in the centrosymmetric space group *Pnnm*. There are three sites for water that are required to be half-occupied by crystallographic symmetry, one site of which is disordered into two oxygen positions. Water hydrogens were not located but were included in the formula. Two half-occupied perchlorate sites with crystallographic symmetry were mod-

* Corresponding author.
*E-mail address:* rdbritt@ucdavis.edu (R. David Britt).

0277-5387/$ - see front matter © 2013 Published by Elsevier Ltd.
http://dx.doi.org/10.1016/j.poly.2013.05.038

eled. Distance restraints were applied for Cl–O and O···O atoms. The structure was an inversion twin, and the twin parameter refined to 0.52(4). See Table 1 for additional details.

### 2.3. High-frequency and -field electron paramagnetic resonance (HFEPR)

HFEPR spectra were recorded at the Electron Magnetic Resonance Facility at NHMFL, Tallahassee, FL. A home-made, single-pass transmission spectrometer differed from the one described in detail in [11] only by the use of a Virginia Diodes (Charlottesville, VA) source operating at 13 ± 1 GHz and followed by a cascade of frequency multipliers. A 15/17 T superconducting magnet and field modulation at 50 kHz was employed. Detection was provided with an InSb hot-electron bolometer (QMC Ltd., Cardiff, UK). A standard lock-in amplifier (Stanford Research Systems SR830) converted the modulated signal to DC voltage. The crystalline sample was dissolved in 1:1 acetonitrile:dichloromethane and placed in a Teflon container. All simulations were performed using the EasySpin 4.5.0 toolbox [12,13] in MatLab (The Mathworks Inc., Natick, MA).

## 3. Results and discussion

In our earlier EPR spectroscopic study of $[Co_4O_4(py)_4(OAc)_4]^+$, we measured the $^{59}Co$ and $^{14}N$ hyperfine coupling interactions using electron-nuclear double resonance (ENDOR) and electron spin-echo envelope modulation (ESEEM) techniques, respectively [5]. The observed $^{59}Co$ hyperfine interaction was relatively small compared to that measured for other $Co^{IV}$-containing systems suggesting that the unpaired electron was significantly delocalized onto other atoms of the molecule. In addition, the ESEEM results could only be properly simulated if four identical $^{14}N$ interactions were employed (i.e. each of the four pyridyl ligands to cobalt experienced the same magnitude of hyperfine interaction). These results suggested that the unpaired electron that should nominally be localized on a $Co^{IV}$-center was actually distributed evenly about all four metal centers. Indeed, this conclusion was further supported by results from density functional theory calculations which predicted that each of the eight core atoms of the cube carried approximately 12% of the unpaired electron spin.

**Table 1**
Crystal data and structure refinement for $[Co^{III}_3Co^{IV}O_4(py)_4(OAc)_4](ClO_4)\cdot 1.5H_2O$.

| | |
|---|---|
| Empirical formula | $C_{28}H_{35}ClCo_4N_4O_{17.5}$ |
| Formula weight | 978.77 |
| $T$ (K) | 90(2) |
| Wavelength (Å) | 0.71073 |
| Crystal system | orthorhombic |
| Space group | $Pmn2_1$ |
| *Unit cell dimensions* | |
| $a$ Å | 13.3347(9) |
| $b$ Å | 20.2024(18) |
| $c$ Å | 13.6960(12) |
| $\alpha$ (°) | 90 |
| $\beta$ (°) | 90 |
| $\gamma$ (°) | 90 |
| $V$ (Å$^3$) | 3689.6(5) |
| $Z$ | 4 |
| $D_{calc}$ (Mg/m$^3$) | 1.762 |
| Absorption coefficient (mm$^{-1}$) | 1.920 |
| $F$(000) | 1984 |
| Crystal size (mm$^3$) | 0.12 × 0.12 × 0.07 |
| Crystal color and habit | green block |
| Diffractometer | Bruker Apex DUO |
| $\theta$ range for data collection (°) | 1.008–29.573 |
| Index ranges | $-18 \leqslant h \leqslant 18$, $-28 \leqslant k \leqslant 28$, $-19 \leqslant l \leqslant 18$ |
| Reflections collected | 56285 |
| Independent reflections $R_{(int)}$ | 10747(0.0517) |
| Observed reflections ($I > 2\sigma(I)$) | 9744 |
| Completeness to $\theta$ = 25.24° | 99.9% |
| Absorption correction | multi-scan |
| Maximum and minimum transmission | 0.746 and 0.685 |
| Solution method | SHELXS-97 [10] |
| Refinement method | SHELXL-2012 (Sheldrick, 2012) |
| Data/restraints/parameters | 10747/41/556 |
| Goodness-of-fit (GOF) on $F^2$ | 1.070 |
| Final $R$ indices [$I > 2\sigma(I)$] | $R_1$ = 0.0881, $wR_2$ = 0.2079 |
| $R$ indices (all data) | $R_1$ = 0.0959, $wR_2$ = 0.2133 |
| Absolute structure parameter | 0.52(4) |
| Extinction coefficient | $n/a$ |
| Largest difference peak and hole (e Å$^{-3}$) | 3.588 and −1.903 |

The results of our X-ray structural and HFEPR studies described below lend further support to this very distributed unpaired electron formulation. In the asymmetric unit of the crystal structure there are two half-clusters residing on the crystallographic mirror plane in the orthorhombic space group $Pmn2_1$. A half-molecule of perchlorate anion balances the charge of the mixed-valent species. In addition, there are three half-molecules of water. Fig. 1 depicts the overall structure, after generation by mirror symmetry, minus the water and hydrogen atoms. The cluster consists of four cobalt ions that form a tetrahedron capped on each face by oxo dianions. The octahedral coordination environment of Co is completed by one pyridine nitrogen and two oxygens from one-half of two bridging acetate groups. As can be seen in the figure, the coordinated pyridine groups exist in a $\pi\cdots\pi$ stacking arrangement in the crystal. Corresponding bonds to the metal centers, as shown in Table 2, do not allow for discrimination of which is $Co^{III}$ and which is $Co^{IV}$.

A comparison of the X-ray structure of oxidized $[Co_4O_4(py)_4(OAc)_4]$ to that previously reported for the all-cobaltic form indicates some small differences [9]. The overall increase in cobalt oxidation state should lead to a decrease in various Co–L bond distances (see for example [14]). Indeed, we observe that the average Co–N internuclear distance contracts slightly by <0.01 Å upon one-electron oxidation. However, changes in Co–O(oxido) distances are more pronounced, shrinking by nearly 0.02 Å. The Co–O(acetate) bond lengths shrink less so (≈0.01 Å), though there appears to be a high degree of variability in this distance (see Table 2) due possibly to crystal packing effects. Interestingly, the set of Co···Co internuclear distances for cobalt ions bridged by one acetate and

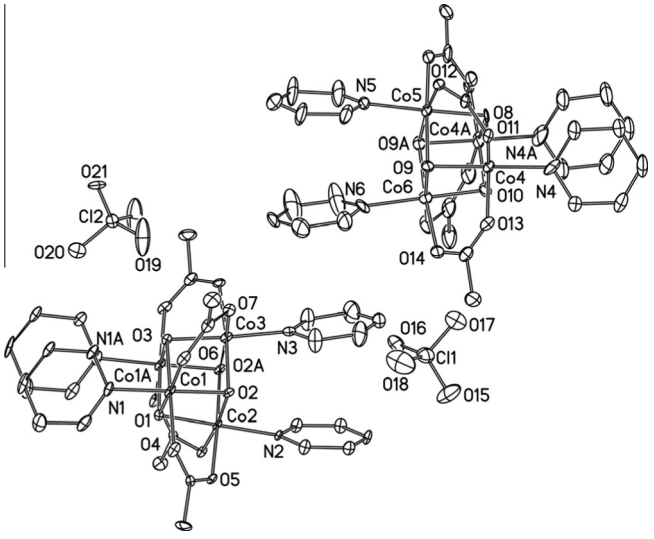


**Fig. 1.** A drawing of the structure of $[Co_4O_4(py)_4(OAc)_4](ClO_4)$ showing displacement parameters at the 35% probability level. Molecules of water and hydrogen atoms are omitted for clarity.

**Table 2**
Selected bond lengths (Å) and angles (°) for the Co environment.

| | | | |
|---|---|---|---|
| *Co–O(oxo)* | | | |
| Co(1)–O(1) | 1.855(7) | Co(4)–O(8) | 1.862(8) |
| Co(1)–O(2) | 1.844(7) | Co(4)–O(9) | 1.881(10) |
| Co(1)–O(3) | 1.871(7) | Co(4)–O(10) | 1.845(9) |
| Co(2)–O(1) | 1.855(10) | Co(5)–O(8) | 1.865(11) |
| Co(2)–O(2) | 1.880(7) | Co(5)–O(9) | 1.870(12) |
| Co(3)–O(2) | 1.871(7) | Co(6)–O(9) | 1.845(13) |
| Co(3)–O(3) | 1.849(10) | Co(6)–O(10) | 1.867(15) |
| *Co–O(OAc)* | | | |
| Co(1)–O(4) | 1.954(8) | Co(4)–O(11) | 1.909(14) |
| Co(1)–O(6) | 1.942(7) | Co(4)–O(13) | 1.923(13) |
| Co(2)–O(5) | 1.947(7) | Co(5)–O(12) | 1.956(12) |
| Co(3)–O(7) | 1.950(7) | Co(6)–O(14) | 1.962(17) |
| *Co–N* | | | |
| Co(1)–N(1) | 1.956(9) | | |
| Co(2)–N(2) | 1.941(12) | | |
| Co(3)–N(3) | 1.956(13) | | |
| Co(4)–N(4) | 1.954(15) | | |
| Co(5)–N(5) | 1.966(17) | | |
| Co(6)–N(6) | 1.958(19) | | |
| *Co–Co* | | | |
| Co(1)–Co(2) | 2.6586(19) | | |
| Co(1)–Co(3) | 2.671(2) | | |
| Co(1)–Co(1)A | 2.811(2) | | |
| Co(2)–Co(3) | 2.831(3) | | |
| Co(4)–Co(6) | 2.670(3) | | |
| Co(4)–Co(5) | 2.678(3) | | |
| Co(4)–Co(4)A | 2.819(7) | | |
| Co(5)–Co(6) | 2.813(3) | | |

Symmetry transformations used to generate equivalent atoms: $A = -x, y, z$.

two oxido ligands shrinks from 2.70 to 2.67 Å while those bridged merely by two oxido groups stay separated by about 2.82 Å. These changes, while small, further support that the removal of an electron has increased selected M–L bond strengths and that the corresponding hole is distributed about the entire cuboidal core. These findings are consistent with those from an earlier crystallographic study of a bipyridine-coordinated analog of the one-electron oxidized cobalt cube in which the equivalent structure of all four cobalt ions pointed to complete "electronic delocalization" [15]. The molecular orbital (MO) in which this hole is housed was computed via density functional theory (DFT) in our earlier study of $[Co_4O_4(py)_4(OAc)_4]^+$.[5] This MO has significant Co–O(oxido) antibonding character so its depopulation upon oxidation should strengthen Co–oxido bonds, a finding consistent with the X-ray structure reported here.

The best-fit simulation of the multifrequency EPR data requires a significantly more axial $g$-tensor than what we previously estimated – originally $g = [2.35, 2.32, 2.06]$ – based on 9 and 34 GHz results alone. The best-fit $g$-values are now [2.3335, 2.3245, 2.0608]. The degree of $g$-anisotropy and the $g$-strain (the full-width at half-maximum variance in the $g$-value due to sample heterogeneity) are fit based on agreement between the highest-frequency data (219.2 GHz, Fig. 2) and the simulation (higher frequencies yielded unsatisfactory signal-to-noise ratios). The linewidth and lineshape of the lower frequency spectra are largely determined by the unresolved hyperfine interactions predominantly of the four $^{59}Co$ ($I = 7/2$) nuclei. The high degree of axiality of the $g$-values revealed by our HFEPR results ($|g_x - g_y| = 0.0090$) is also more consistent with the DFT-predicted magnetic parameters ($|g_x - g_y| = 0.002$ in the fully geometry-optimized model and $|g_x - g_y| = 0.020$ in the model based on the X-ray structure of the reduced cluster) [5]. As described in a study of a mixed-valence dinuclear Cu spin system [16], the molecular (observed) $g$-anisotropy is determined by geometric relationships between the site-specific $g$-matrix on each spin-carrying center. The lack of a significant difference between $g_x$ and $g_y$ observed here for $[Co_4O_4(py)_4(OAc)_4]^+$ is indicative of each of the four cobalt sites being aligned to cancel out any anisotropy in the site $g$-matrix. Detailed equations for this procedure are provided in the Supporting Information of our earlier study [5].

Collectively, these geometric and electronic structure results for $[Co_4O_4(py)_4(OAc)_4]^+$ lend further support to our original electronic structure description of the oxidized tetranuclear cobalt cube. Importantly, the pulse EPR and HFEPR measurements performed to-date have been done so using solutions in aprotic solvents (e.g. 1:1 acetonitrile:dichloromethane). Our interpretation of the earlier ESEEM results showed that four pyridine nitrogens were coupled to the unpaired electron in equivalent fashion. The water-oxidizing activity reported for this and related cobalt-oxido cuboidal species [6–8], strongly indicates that at least one ligand must dissociate to allow for the substrate water molecule(s) to coordinate. The high degree of axiality measured here for $[Co_4O_4(py)_4(OAc)_4]^+$ reflects the high geometric symmetry of the cube and that the unpaired spin is so evenly delocalized. Ligand dissociation would break the symmetry of the cubane and is expected to have a dramatic affect on the EPR spectrum. Future EPR studies of the $[Co_4O_4(py)_4(OAc)_4]^+$ generated in aqueous solutions are expected to reveal great insight into the nature of such structural changes

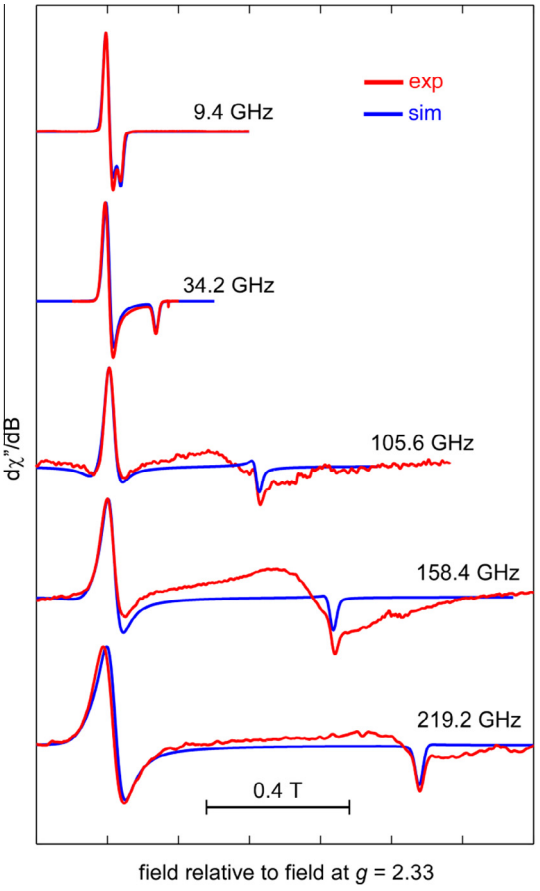


**Fig. 2.** Multifrequency EPR spectra of $[Co_4O_4(py)_4(OAc)_4]^+$. The EPR spectra with excitation frequencies of 9.40 and 34.20 GHz were collected at CalEPR and are reproduced here from an earlier publication. The remaining, higher frequency data (excitation frequencies noted in figure) were collected at the NHMFL. The overlaid simulations were generated using the following parameters: $g = [2.3333\ 2.3245\ 2.0608]$, $g$-strain = [0.0357 0.0117 0.00525], $H$-strain = [645 615 408] MHz. A Voigtian lineshape was used with peak-to-peak width of 3.2 and 1.0 mT for the Gaussian and Lorentzian contributions, respectively. Since the HFEPR spectra show an admixture of dispersion, a Voigtian broadening was employed to account for it. The necessary phase correction was: $-43(\pm3)°$, $-15(\pm3)°$, and $6(\pm3)°$ for 105.6, 158.4, and 219.2 GHz simulations, respectively. The origin of the broad, derivative-shaped signal centered at $g \approx 2$ is unknown and the signal is not simulated.

and further aid in our understanding of the $Co^{IV}$ species formed in cobalt-oxide films under oxidizing conditions [17].

## Acknowledgements

This research was supported by a National Science Foundation grant EAR0814242 and by the US Department of Energy Office of Basic Energy Science under grant DEFG03–02ER15693 (to W.H.C) and NSF grant CHE-0939178 and CHE-1213699 to R.D.B. Part of the work was done at the National High Magnetic Field Laboratory, which is funded by NSF (Cooperative Agreement DMR 1157490), the State of Florida, and DOE.

## Appendix A. Supplementary data

CCDC 931735 contains the supplementary crystallographic data for $[Co^{III}_3Co^{IV}O_4(py)_4(OAc)_4](ClO_4)\cdot 1.5H_2O$. These data can be obtained free of charge via http://www.ccdc.cam.ac.uk/conts/retrieving.html, or from the Cambridge Crystallographic Data Centre, 12 Union Road, Cambridge CB2 1EZ, UK; fax: +44 1223 336 033; or e-mail: deposit@ccdc.cam.ac.uk. Supplementary data associated with this article can be found, in the online version, at http://dx.doi.org/10.1016/j.poly.2013.05.038.

## References

[1] M.W. Kanan, D.G. Nocera, Science 321 (2008) 1072.
[2] J.G. McAlpin, Y. Surendranath, M. Dinca, T.A. Stich, S.A. Stoian, W.H. Casey, D.G. Nocera, R.D. Britt, J. Am. Chem. Soc. 132 (2010) 6882.
[3] M. Risch, V. Khare, I. Zaharieva, L. Gerencser, P. Chernev, H. Dau, J. Am. Chem. Soc. 131 (2009) 6936.
[4] M.W. Kanan, J. Yano, Y. Surendranath, M. Dincă, V.K. Yachandra, D.G. Nocera, J. Am. Chem. Soc. 132 (2010) 13692.
[5] J.G. McAlpin, T.A. Stich, C.A. Ohlin, Y. Surendranath, D.G. Nocera, W.H. Casey, R.D. Britt, J. Am. Chem. Soc. 133 (2011) 15444.
[6] G. La Ganga, F. Puntoriero, S. Campagna, I. Bazzan, S. Berardi, M. Bonchio, A. Sartorel, M. Natali, F. Scandola, Faraday Discuss. 155 (2012) 177.
[7] N.S. McCool, D.M. Robinson, J.E. Sheats, G.C. Dismukes, J. Am. Chem. Soc. 133 (2011) 11446.
[8] S. Berardi, G. La Ganga, M. Natali, I. Bazzan, F. Puntoriero, A. Sartorel, F. Scandola, S. Campagna, M. Bonchio, J. Am. Chem. Soc. 134 (2012) 11104.
[9] R. Chakrabarty, S.J. Bora, B.K. Das, Inorg. Chem. 46 (2007) 9450.
[10] G.M. Sheldrick, Acta Crystallogr., Sect. A 64 (2008) 112.
[11] A.K. Hassan, L.A. Pardi, J. Krzystek, A. Sienkiewicz, P. Goy, M. Rohrer, L.C. Brunel, J. Magn. Reson. 142 (2000) 300.
[12] S. Stoll, R.D. Britt, Phys. Chem. Chem. Phys. 11 (2009) 6614.
[13] S. Stoll, A. Schweiger, J. Magn. Reson. 178 (2006) 42.
[14] R.A. Lewis, S.P. George, A. Chapovetsky, G. Wu, J.S. Figueroa, T.W. Hayton, Chem. Commun. 49 (2013) 2888.
[15] K. Dimitrou, A.D. Brown, T.E. Concolino, A.L. Rheingold, G. Christou, Mixed-valence, tetranuclear cobalt(III, IV) complexes: preparation and properties of $[Co_4O_4(O_2CR)(2)(bpy)(4)](3+)$ salts, Chem. Commun. (2001) 1284.
[16] F. Neese, W.G. Zumft, W.E. Antholine, P.M.H. Kroneck, J. Am. Chem. Soc. 118 (1996) 8692.
[17] J.B. Gerken, J.G. McAlpin, J.Y.C. Chen, M.L. Rigsby, W.H. Casey, R.D. Britt, S.S. Stahl, J. Am. Chem. Soc. 133 (2011) 14431.